Centriole Loss in Embryonic Development Disrupts Axonal Pathfinding and Muscle Integrity

Beatriz González[1,2], Júlia Sellés-Altés[1], Jèrica Pla-Parron[1], Judith Castro-Ribera[1], and Sofia J. Araújo*[1,2]

[1]Department of Genetics, Microbiology and Statistics, Facultat de Biologia, Universitat de Barcelona (UB), 08028 Barcelona, Spain

[2]Institut de Biomedicina Universitat de Barcelona (IBUB), Barcelona, Spain

*Corresponding author. email: S. J. Araújo sofiajaraujo@ub.edu,

Keywords: centriole; centrosome; axon; nervous system; muscle; Drosophila; Sas-4; Sas-6; wiggliness, tortuosity

Running title: centriole loss disrupts axon and muscle development

Abstract

Centrosomes, the primary microtubule-organizing centers (MTOCs), are crucial for early neuronal development, particularly in establishing polarity and promoting axon formation. Traditionally considered non-essential in terminally differentiated cells, recent evidence suggests that centrosomes play vital roles in specialized cellular contexts. In mammalian neurons, centrosome-mediated microtubule remodeling is essential for axon elongation, with centrosome dysfunction leading to axonal misrouting and growth defects. Although active centrosomes have been detected in the tracheal terminal cells of *Drosophila melanogaster*, their activity in neurons *in vivo* has not been observed. Their gradual loss during embryogenesis has been reported as non-essential for organogenesis, as adult flies can eclose without centrioles.

To investigate centrosome activity in neurons, we revisited *Drosophila Sas-4* mutants, which exhibit centrosome loss (CL), and observed that 50% of homozygous mutant individuals fail to hatch as larvae. We analysed their development, focusing on the expressivity and penetrance of nervous system phenotypes, and examined centriole localization in neurons. Our findings confirm the presence of centrosomes in motor and sensory neurons in *Drosophila* and their localization near the nascent axon. CL conditions resulted in axonal misrouting and muscle developmental abnormalities. Targeted downregulation of Sas-4 in the pioneer motor neurons aCC and RP2 induced axon guidance errors, indicating an autonomous role for centrosomes in axonal navigation. Colocalization of acetylated- and γ-tubulin with centrioles in motor neurons further confirmed the presence of functional centrosomes in these cells. Analysis of motor axons revealed that CL leads to axonal tortuosity, a characteristic associated with neurodegeneration. This is the first direct association of CL with axonal morphological phenotypes, highlighting the role of centrosomes in neuronal development and their broader influence on nervous system structure and function.

Introduction

Centrosomes are small membrane-less organelles that serve as primary microtubule-organizing centres (MTOCs). Composed of a mother-daughter centriole pair surrounded by pericentriolar material (PCM), they anchor and nucleate microtubules (MTs) through γ-tubulin ring complexes (γ-TuRCs) (Bettencourt-Dias & Glover, 2007). During mitosis, centrosomes organize the spindle apparatus, while their role in interphase is more variable (Conduit *et al*, 2015). Abnormalities in centrosomes are linked to disorders like microcephaly and neurodevelopmental disorders, highlighting the importance of centrosome function in early neurodevelopment (Goundiam & Basto, 2020; Marthiens *et al*, 2013). However, how centrosome numbers affect differentiated cells and their involvement in post-cell-division organogenesis is not yet fully understood. Although traditionally studied in dividing cells, recent insights suggest centrosomes also regulate cellular behaviours in differentiated cells,

contradicting the assumption that centrosome-based MTOCs are largely inactive in such contexts.

In vertebrates, centrosomes are critical for embryonic development. For example, null mutations in mouse *Cenpj* (also called *Sas4*) lead to centriole loss and embryonic arrest at embryonic day 9, and *Sass6*-mutant mouse embryos arrest at mid-gestation (Bazzi & Anderson, 2014; Grzonka & Bazzi, 2024). In contrast, *Drosophila melanogaster* embryos have been reported to develop to adulthood using maternally supplied Sas-4 and Sas-6, despite gradual centrosome loss (CL) (Basto *et al*, 2006; Fatalska *et al*, 2021; Gogendeau & Basto, 2010). However, these adults are sterile, uncoordinated, unable to form cilia, and die shortly after eclosion (Basto *et al.*, 2006). Without maternal Sas-4, Sas-4 and Asterless (Asl) *Drosophila* embryonic development arrests early (Stevens *et al*, 2007; Varmark *et al*, 2007), as observed in *C. elegans Sas-4* mutants (Leidel & Gönczy, 2003). In *Drosophila* neural progenitor and epithelial cells, centrosome absence impairs spindle assembly and orientation, leading to defects like neural apoptosis and altered brain size, mimicking either human microcephaly or tumourigenesis (Basto *et al.*, 2006; Castellanos *et al*, 2008; Poulton *et al*, 2014; Poulton *et al*, 2017).

Centrosomes are also important for differentiated cellular functions. In mouse fibroblasts, myoblasts and endothelial cells, centrosome orientation is important for nuclear positioning and cell migration(Chang *et al*, 2015; Gomes *et al*, 2005; Kushner *et al*, 2014). During kidney development, CL leads to decreased branching morphogenesis and small dysplastic kidneys at birth (Cheng *et al*, 2023). In *Drosophila* tracheal terminal cells (TCs), centrosome numbers influence the formation of subcellular lumina during tubulogenesis (Ricolo *et al*, 2016). Increasing centrosome numbers or depleting centrosomal proteins alters this process, stressing their importance in cells with specialized architectures (Ricolo *et al*, 2021).

In neurons, centrosomes play critical roles as MTOCs during early development, particularly in axon formation, a process reliant on microtubule remodelling to establish neuronal polarity (Meka *et al*, 2022). In mammalian neurons, centrosomes nucleate MTs in the soma, which are subsequently severed and transported into neurites via motor-driven sliding, enabling axon

elongation and polarity establishment (Ahmad & Baas, 1995; del Castillo *et al*, 2015; Stiess *et al*, 2010; Yu *et al*, 1993). In hippocampal neurons *in vitro,* suppression of centrosome-mediated functions prevents axonal growth and neurons with more than one centrosome sprout more than one axon (Anda *et al*, 2005). In addition, aberrant centrosome localization, leads to misplaced axonal outgrowth(Anda *et al*, 2010). In human iPSC-derived neurons, depleting centrioles causes significant axonal defects, including mislocalization of axonal MT-associated proteins and affected growth cone morphologies (Lindhout *et al*, 2021). However, as neurons mature, γ-tubulin (γ-tub) remains essential, but centrosomes lose MTOC activity and become dispensable in mammals and flies (Leask *et al*, 1997; Nguyen *et al*, 2011; Sanchez-Huertas *et al*, 2016; Stiess *et al.*, 2010).

These findings collectively suggest that while centrosomes are essential in specific cells, stages and contexts, many differentiated cells can adapt to their loss through alternative MTOCs. However, in many cases, CL induces phenotypes which indicate its important function in cytoskeletal remodelling and the acquisition of specialised cell shapes (Araújo, 2019).

To investigate the role of centrosomes in neuronal development, we revisited *Drosophila Sas-4* mutants with reduced centriole numbers and analysed their embryonic development. We quantified the expressivity and penetrance of nervous system phenotypes and examined centriole localization within neurons. Our findings indicate that loss of centrosomal protein function results in variable expressivity and penetrance of embryonic phenotypes, which likely accounts for inconsistencies in previously reported results. We observed that centrosomes are present and active in *Drosophila* motor and peripheral nervous system (PNS) neurons. Importantly, CL during embryogenesis leads to axonal misrouting and abnormalities in muscle development, emphasising a critical role of centrosomes in proper nervous system and muscle structure formation. Furthermore, we were able to specifically observe axonal phenotypes associated with CL.

Results

Sas-4 mutant conditions induce axonal misrouting phenotypes

Spindle assembly abnormal 4 (Sas-4) protein is essential for centriole replication in *Drosophila* and early embryonic development (Basto *et al.*, 2006; Stevens *et al.*, 2007). However, in contrast to *Sas-4* maternal mutants, *Sas-4* zygotic mutant embryos initially progress through early development due to the maternal contribution but gradually lose centrioles during embryonic and larval stages. This progressive centriole loss makes these mutants an excellent model for studying the role of centrosomes in differentiated cells. By embryonic stages 15–16, centrioles have reported to be undetectable in 50–80% of cells (Basto *et al.*, 2006). By these stages, *Sas-4* mutant embryos exhibit defects in tracheal subcellular lumen formation, showing the importance of centrioles in some differentiated cells (Ricolo *et al.*, 2016). Nevertheless, *Sas-4* homozygous mutants have been reported to survive to adulthood, exhibiting early lethality shortly after eclosion(Basto *et al.*, 2006). This early adult lethality suggests a critical role for Sas-4 in maintaining cellular and developmental processes essential for organismal viability.

To investigate the role of centrosomes in embryonic development, we first analysed the viability of *Sas-4* loss-of-function (LOF) mutants during embryonic, larval and adult stages. As previously reported, we were able to raise *Sas-4* mutant adults; however, only a proportion of Sas-4 individuals were found to eclose. These mutants were uncoordinated and became trapped in the food upon eclosion. When isolated at the pupal stage and placed in Petri dishes, they were able to eclose and survive for longer, but with available food, they died within 24-36 hours, which is significantly less than the reported survival rates of unfed flies (2-3 days) (Kopeć, 1928; Pearl & Parker, 1921). These adult individuals exhibited severe motor impairments, barely moving and failing to extend their wings (Fig. 1A). To obtain survival rates, we quantified the percentage of *Sas-4* mutants that reached adulthood, compared to the total number expected, based on Mendelian proportions from a cross between heterozygous *Sas-*

137 *4/TM3ftzlacZ* individuals. Since the homozygous balancer chromosome embryos are early
138 embryonic lethal, we could detect a proportion of 33.3% mutant embryos reaching embryonic
139 stage 16. However, we only detected 16.7% of L1 larvae 36h after egg laying (AEL) (Fig. 1B,
140 n=407). This proportion was maintained to wandering L3, pupal and adult stages, suggesting
141 that once the barrier of embryonic stages is passed, centrosomes are no longer necessary for
142 viability, and individuals can reach adult stages as previously reported (Basto *et al.*, 2006).
143 However, our results show that only 50% of the homozygous embryos successfully reached
144 the larval and adult stages, indicating that CL induces embryonic lethality in the remaining
145 50% of cases.
146 We then asked if the *Sas-4* embryos exhibited mutant nervous system phenotypes. To do so,
147 we first analysed FasII positive neurons focusing on the trajectories of their motor axons,
148 particularly on the Intersegmental Nerve (ISN) (Fig. 1C). The penetrance of the ISN phenotype
149 was 52.8% (n=53) quantified as at least 2 defects per embryo, despite variability in the
150 expressivity of the phenotype (Fig. 1E and H and Sup. Fig. 1B). The aberrant pathways
151 included the following: synaptic phenotypes, which were evident when the nerve fibres
152 innervated the wrong target or failed to innervate (Fig. 1E and Sup. Fig. 1B, arrow); misrouting
153 phenotypes, which involved defects in nerves that do not follow the wild-type (wt) stereotypical
154 routes (Fig. 1E and Sup. Fig. 1B, asterisk); and crossing phenotypes, which included aberrant
155 crossing between segments (Fig. 1E arrowhead). The same type of anomalous phenotypes
156 was detected in *Sas-4/Df* mutant embryos (Fig. 1F and H), penetrance 56% (n=25), as well
157 as RNAi Sas-4 downregulation (Fig. 1G and H), penetrance 33.3% (n=15). We downregulated
158 Sas-4 using a *UAS-Sas-4RNAi* expressed in all post-mitotic neurons, by an elavGal4 driver
159 (Sup. Fig. 1 D and K) and specifically in a subset of neurons, such as the anterior corner cell
160 (aCC), posterior corner cell (pCC) and RP2 pioneers, using RN2-Gal4 (Fujioka *et al*, 2003).
161 Interestingly, when Sas-4 was specifically downregulated in neurons, we observed an
162 additional phenotype: fasciculation/defasciculation defects (Fig. 1G arrow) ISN misrouting and
163 defasciculation phenotypes (Fig. 1G and Sup. Fig. 1D, asterisk and arrowhead) as well as
164 shorter nerve extensions (Fig. 1 G, dot), also observed in some *Sas-4* and *Sas-4/Df* mutant

165 embryos (Fig. 1F' and Sup. Fig. 1 C). This suggested these motor axon phenotypes were
166 induced cell-autonomously. Furthermore, ubiquitous expression of *Sas-4* using a *pUbqSas-4*
167 insertion (Peel *et al*, 2007), could partially rescue the mutant phenotypes, particularly by
168 reducing the number of defects (Fig. 1 H and Sup. Fig. 1 E and K).
169 We followed by analysing the peripheral nervous system (PNS) phenotypes of *Sas-4* mutant
170 conditions specifically focusing on their axonal misrouting phenotypes. We could detect axonal
171 misrouting phenotypes in all three mutant conditions: *Sas-4* (penetrance 60% n=20), *Sas-4/Df*
172 (penetrance 55% n=20) and *UAS-Sas-4RNAi* (penetrance 60% n=20) (Fig. 1J-L and M)
173 expressed in PNS neurons using *P0163Gal4* (Hummel *et al*, 2000). We could partially rescue
174 these phenotypes by expressing *Sas-4* ubiquitously (Fig.1M and Sup. Fig. 1J and L). Taken
175 together, these results indicate that *Sas-4* conditions lead to mutant phenotypes in the nervous
176 system, characterized by incomplete penetrance and variable expressivity. These phenotypes
177 appear to be at least partially cell-autonomous, as Sas-4 downregulation in motor and sensory
178 neurons results in axonal misrouting errors.
179
180 ***Sas-4* mutant conditions disrupt muscle development**
181 Since the phenotypes induced by RNAi expression exclusively in neurons did not fully replicate
182 the strength of the motor axon defects observed in *Sas-4* embryos, we next decided to
183 investigate the muscle phenotypes in *Sas-4* mutants. Muscles play a critical role in guiding
184 motor neurons by providing chemical and physical cues essential for accurate axonal
185 pathfinding and target selection (Jeong, 2021). These signals ensure proper neuromuscular
186 connections, essential for coordinated movement. In *Drosophila* mutants lacking muscular
187 structures, such as *twist* (*twi*) embryos, the absence of these cues disrupts motor axon
188 trajectories (Younossi-Hartenstein & Hartenstein, 1993).
189 In stage 16 *Drosophila* embryos, each abdominal hemisegment (A2–A7) displays a consistent
190 and repeating pattern of 30 somatic muscle fibres, which can be visualized using a myosin-
191 specific antibody (Fig. 2A and C). These 30 syncytial muscle fibres are innervated by two

192 motor nerves: the anterior ISN, which targets the dorsal muscles, and the posterior SN, which
193 innervates the ventral muscles (Fig. 2C, wt). We first analysed the muscle pattern of *Sas-4*
194 mutant embryos and could detect defects that ranged from misplaced to missing muscle fibres
195 (Fig. 2 B, B´). We then analysed these muscle fibre phenotypes in parallel to the axonal defects
196 and were able to correlate many of the axonal defects in *Sas-4* embryos to the location of the
197 muscle pattern disruptions (Fig. 2E'' and Sup. Fig. 2B', asterisk). In fact, 100% of *Sas-4*
198 embryos with detectable muscle mutant phenotypes also exhibited ISN axonal trajectory
199 disruptions, while 11% of embryos displayed ISN axonal misrouting without any observable
200 muscle phenotypes (n = 27). Accordingly, Sas-4 downregulation in muscle cells, using a *Mef2*
201 driver, induced muscle mutant phenotypes in 80% of embryos, with ISN defects spatially
202 correlating with muscle defects in 63% of the cases (n = 19, Fig. 2G'' asterisk). Sas-4
203 downregulation in muscle cells, using a *Mef2* driver together with a *Twist* (*Twi*) driver, induced
204 stronger, more penetrant ISN phenotypes that were dose dependent (Sup. Fig. 2E, F)
205 Consistent with these findings, downregulation of Sas-4 in pioneer neurons using the RN2
206 driver resulted in axonal misrouting phenotypes in 33% of the embryos (n = 15) and very mild
207 muscle mutant phenotypes in only 20% of the embryos (n = 10). Collectively, these findings
208 suggest that axonal misrouting phenotypes arise from two distinct contributions: an
209 autonomous component originating from their own CL and a non-autonomous one driven by
210 CL-affected muscle cells (Fig. 2C, *Sas-4*).
211

212 ***Sas-6* mutants have axonal guidance and muscle developmental defects**

213 Centriole assembly depends on a small set of conserved proteins, the absence of any of which
214 results in centriole loss; *Sas-4* and *Sas-6* are key components of this process (Gartenmann *et*
215 *al*, 2020). To rule out the possibility that the observed axonal and muscle defects were
216 specifically due to mutations in *Sas-4*, we began by analysing the viability of *Sas-6* LOF
217 mutants during the embryonic, larval, and adult stages. We used a transallelic combination of
218 two CRISPR-Cas9 generated *Sas-6* induced deletions mutants, $Sas\text{-}6^{\Delta a}/Sas\text{-}6^{\Delta b}$ (Z. Novak

219 and J. Raff, unpublished). We successfully raised *Sas-6* adults (Fig. 3A), which, like *Sas-4*
220 adults, died within 24-36 hours. To corroborate that this combination of *Sas-6* alleles induced
221 CL in embryos, we counted the number of centrioles in *Sas-6*$^{\Delta a}$/*Sas-6*$^{\Delta b}$ embryos and observed
222 a reduction at stage 16 (Fig. 3B). Like *Sas-4* mutants, 33.3% of *Sas-6* mutant embryos
223 reached embryonic stage 16. However, compared to *Sas-4* mutants, in *Sas-6* we observed a
224 higher survival rate of 27.5% at the L1 larval stage (Fig. 3C, n=407). This proportion was
225 maintained through the wandering L3, pupal, and adult stages, suggesting that, like in *Sas-4*
226 mutants, centrosomes seem not to be essential for larval and pupal development once the
227 embryonic stages are completed.
228 We then investigated whether *Sas-6* embryos exhibited mutant axonal guidance and muscle
229 phenotypes. We then investigated whether *Sas-6* embryos exhibited mutant axonal guidance
230 and muscle phenotypes. We observed ISN axonal misrouting in *Sas-6* embryos (Fig. 3E, F),
231 with a penetrance of 47.6% (n=20), similar to that seen in *Sas-4* embryos. However, the
232 severity of the defects was milder than in *Sas-4*, as we did not observe any strong axonal
233 misrouting or crossing phenotypes. In most cases, the ISN axonal misrouting also correlated
234 with muscle phenotypes (Fig. 3E'' and F'', asterisk). Altogether, these findings support the role
235 of centrosomes in regulating axon guidance of motor neurons.
236
237 **Pioneer neurons have centrioles localizing to the sites of axon outgrowth**
238 In *Drosophila*, the aCC and RP2 motor neurons are pioneer neurons which influence growth
239 of the ISN (Sánchez-Soriano & Prokop, 2005) (Fig. 4 A). Pioneer neurons extend growth cones
240 that navigate a future fibre tract, and must interpret the full complexity of environmental cues
241 to define the path of the nerve (Harrison, 1910; Jacobs & Goodman, 1989). Therefore, we
242 investigated whether centrioles could be detected in the soma of these neurons in stage 12-
243 13 when they are starting to extend their axons. We found that centrioles were present in the
244 soma of both aCC (Fig. 4 B and C) and RP2 motor neurons (Fig. 4 D). Specifically, in the case
245 of the aCC, a centriole was observed in the quadrant where the axon exit point is first detected
246 in 72% of the cases (Fig. 4B n=75). Additionally, we did not detect centrioles in the quadrant

247 opposite the axon exit point (Fig. 2B n=75). In *Sas-4* mutants, centrioles were largely
248 undetected in both aCC/pCC neurons and RP2 neurons. (Fig. 4 E, F). At these stages, the
249 aCC and pCC neurons are very close together, making it difficult to differentiate between the
250 somas of the two neurons. Therefore, we quantified the number of centrioles in aCC+pCC and
251 RP2 neurons in both control and *Sas-4* mutant embryos. In control embryos, we observed
252 around 2.53 centrioles per pair of aCC and pCC neurons, while in *Sas-4* mutant, this number
253 was significantly reduced to 0.81 (Fig. 4G n=76). Similarly, for RP2 neurons, control embryos
254 exhibited 0.81 centriole per RP2 neuron, whereas *Sas-4* embryos showed a reduction to 0.26
255 (Fig. 4G n=76). This significant decrease in the humber of centrioles further supports the
256 critical role of Sas-4 in pioneer neurons of the ventral nerve cord (VNC) during *Drosophila*
257 embryogenesis.
258
259 **Non-ciliated sensory neurons have centrioles**
260 In *Drosophila* embryos, the dorsal cluster neurons project their axons in a highly organized
261 manner to form the sensory axonal tracts (Ghysen *et al*, 1986). During development, the axons
262 of these neurons extend dorsally and medially, connecting with their target regions and
263 fasciculating with the intersegmental nerve (ISN) to form a bundled tract for efficient sensory
264 signal routing (Hartenstein, 1988). Sensory neurons in *Drosophila* embryos are known to have
265 centrioles. These centrioles are crucial for forming basal bodies in ciliated cells, including type-
266 I sensory neurons, which are essential for the development of cilia (Jana *et al*, 2016). Since
267 we detected axonal guidance phenotypes in the axons extending from the dorsal cluster, we
268 tested for the presence of centrioles in dorsal cluster sensory neurons (Fig. 5A). We detected
269 centrioles in the soma of most of these neurons and quantified the number of centriole-positive
270 ddaC neurons (Fig. 5A", B, and C', arrowhead), finding centrioles in 81.4% of the total (Fig.
271 5B, n=43). Importantly, we also detected centrioles in dorsal bipolar neuron (dbp, also known
272 as dbd), the proposed pioneer neuron of the dorsal cluster (Fig. 5A" and C', arrow) (Martin *et*
273 *al*, 2008; Merritt & Whitington, 1995). In *Sas-4* embryos, the presence of centrioles in the

274 dorsal cluster neurons was significantly lower (Fig. 5D). In many embryos, we could not detect
275 any centrioles in the soma of the dorsal cluster neurons (Fig. 5E).
276 Based on our findings in the CNS and PNS, we decided to quantify the total number of
277 centrioles in *Sas-4* embryos and compare them to controls. To do so, we selected equal
278 segmental areas spanning the dorsal cluster and the lateral chordotonal organs (lch) and
279 counted the total number of centrioles in stage 16 control embryos, *Sas-4* homozygous
280 embryos displaying the mutant phenotype, *Sas-4* homozygous embryos with no mutant
281 phenotype and *Sas-4* mutants rescued by ubiquitous Sas-4 expression (Fig. 5F). We observed
282 that both mutants had approximately one-third of the centrioles found in the control group.
283 Embryos without defects had slightly higher centriole numbers compared to those with mutant
284 phenotypes. Additionally, ubiquitous expression of Sas-4 could increase centriole numbers.
285 These results confirm that *Sas-4* embryos gradually lose their centrioles. Significantly, we also
286 found a correlation between axonal guidance phenotypes and the numbers of centrioles per
287 embryo.
288
289 **Pioneer motor neurons have active centrosomes**
290 After revealing that ISN pioneers have centrioles, we were interested in knowing if these could
291 be active MTOCs. To determine if the centriole could organize a functional centrosome and
292 serve as a major site of neuronal microtubule nucleation in aCC and RP2 neurons, we
293 analysed the localization of acetylated-tubulin (ace-tub) and γ-tubulin (γ-tub). MTs are
294 nucleated and anchored by the microtubule nucleator γ-tub, which is embedded within the
295 pericentriolar material (PCM) of the centrosome (Lin *et al*, 2015). In both neurons we could
296 see stable acetylated MTs extending from the centrosomes (Fig. 6 A, B, arrowheads) and
297 these colocalized with γ-tub (Fig. 6C, D, arrowheads). We quantified the number of centrioles
298 colocalizing with γ-tub (Fig. 6E) and could detect co-localization in 50% of the cases, meaning
299 that there are centrioles in these neurons which are not active as MTOCs at these stages (Fig.

300 6C'' asterisk). In conclusion, these results suggest that at least some microtubule organization
301 in pioneer neurons of the VNC is dependent on the centrosome.
302
303 **Centrosome loss induces motor axon fibre tortuosity**
304 Axonal tortuosity (wiggliness) is a measure of the irregularities or abnormalities in the
305 morphological structure of axons which can be associated with neurodegeneration (Bando *et*
306 *al*, 2015). When axons are "wiggly," it suggests that they are not following their usual straight
307 or organized paths, possibly due to changes in axonal cytoskeletal structure or cell-adhesion,
308 but not much is known about what triggers axonal wiggliness. Qualitative examination of
309 confocal projections showed that aCC and RP2 axons are straighter in controls than in *Sas-4*
310 mutants, revealing the tortuosity of these axons (Fig. 7 A-E, asterisks). Apart from the
311 previously characterised phenotypes such as axonal crossings (Fig. 7 B, arrowhead) and
312 misrouting, we could observe axonal wiggliness at the CNS exit points (Fig. 7 B', D and E,
313 asterisks). Since we were interested in determining the proportion of wiggly axons in the
314 mutant, we quantified this for the aCC and RP2 neurons (Fig. 7 F). In *Sas-4* mutants we could
315 detect an average of 23% aCC and 30% RP2 wiggly axons per total number of aCC and RP2
316 axons, which was significantly different from the proportion of wiggly axons in the controls (6%
317 wiggly aCC and 8% wiggly RP2 axons). Therefore, CL induces axonal morphological changes
318 (Fig. 7G). Most importantly, we could observe specific axonal phenotypes in embryos with
319 reduced centriole numbers, confirming the importance of the centrosome for axonal extension.
320
321 **Discussion**
322 Here we provide evidence that the centrosome plays a role in axonal extension, navigation,
323 and muscle development *in vivo*. Previous studies have shown that *Sas-4* and *Sas-6* mutant
324 flies can reach adulthood (Basto *et al.*, 2006; Fatalska *et al.*, 2021; Peel *et al.*, 2007), which
325 initially seems incompatible with an important role for the centrosome during embryonic

326 development. However, we found that *Sas-4* homozygous mutations result in 50% lethality,
327 and a *Sas-6* transallelic combination causes 17% embryonic lethality.
328 *Sas-4* and *Sas-6* LOF embryos display motor axon mutant phenotypes (Fig. 1 and 3),
329 revealing that centrosomes are important for axonal guidance. Additionally, *Sas-4* and *Sas-6*
330 LOF embryos exhibit muscle mutant phenotypes (Fig. 2 and 3), indicating that centrosomes
331 are also important for muscle development. Hence, the embryonic axon guidance phenotypes
332 have a dual contribution: an autonomous one from axonal CL and a non-autonomous one from
333 muscle CL. Since innervation does not influence the patterning, morphogenesis, maintenance,
334 or physiological development of somatic muscles in *Drosophila* embryos, the muscle defects
335 observed are most likely due to CL in muscle cells (Broadie & Bate, 1993). CL in muscle cells
336 may impair cilia formation and nuclear positioning, two processes important for muscle fibre
337 development (Loh *et al*, 2023; Metzger *et al*, 2012; Tillery *et al*, 2018). Expressing *Sas-4 RNAi*
338 under the control of the muscle-specific *Mef2-GAL4* driver induced penetrant muscle
339 phenotypes, consistent with previous results reporting the lethality of these embryos
340 (Schnorrer *et al*, 2010). *Sas-6* embryos exhibited milder muscle phenotypes than *Sas-4*,
341 aligning with previous findings that driving *Sas-6 RNAi* with a Mef2-GAL4 driver induced adult
342 pharate lethality (Schnorrer *et al.*, 2010).
343 What could explain the variability in the consequences of CL during embryonic development?
344 Many disease-causing mutations exhibit mild or no effects in some individuals, a phenomenon
345 known as incomplete phenotype penetrance. This phenomenon is still poorly understood, but
346 recent studies in *Drosophila* suggest it is stochastic, akin to flipping a coin (Marmion *et al*,
347 2023). Although the reported study focuses on fluctuations in signalling, a similar scenario
348 could be imagined for centrosomes. In cases of centrosome duplication impairment which
349 induce CL, distribution would vary among dividing cells as development proceeds. Early
350 embryonic mitotic cycles can partly explain the differences in phenotype expressivity. The first
351 13 mitotic cycles of *Drosophila* embryos are rapid, synchronous, and occur without cell
352 division. Subsequently, three rounds of patterned mitosis occur (mitoses 14, 15, and 16).
353 Following mitosis 16, many cells enter their first G1 phase (Edgar & O'Farrell, 1990). However,

354 the nervous system lineage does not enter a terminal interphase after mitosis 16 and
355 continues to divide according to an independent program (Bodmer & Jan, 1987; Hartenstein
356 *et al*, 1987). Similarly, muscle cells, continue dividing until embryonic stage 10 (Nabel-Rosen
357 *et al*, 2005). These extra cell divisions can account for the appearance, variability and severity
358 of the phenotypes observed, as centrosome loss is exacerbated with each cell division, which
359 depletes the maternal contribution. In agreement with this, when we quantified the number of
360 centrioles present in *Sas-4* embryos displaying axonal phenotypes, we could detect a
361 decrease of about 1/3 (Fig. 5), with consistent results when we quantified the numbers of
362 centrioles in *Sas-4* aCC, pCC and RP2 neurons (Fig. 4)
363
364 **Centrosome localization in neurons and implications for axonal morphology**
365 Here we show that centrioles are present in motor and sensory neurons and that in motor
366 neurons these centrioles colocalize with acetylated- and γ-tubulin suggesting they are active
367 MTOCs in these cells (Fig. 4, 5 and 6). Previous studies failed to detect colocalization of
368 centrosomes with γ-tub in neurons (Nguyen *et al.*, 2011). However, this study used Fizzy-
369 related-GFP (Fzr-GFP) to visualise centrioles and while it is clear Fzr is localizes to centrioles
370 during the cell cycle (Meghini *et al*, 2016), it is not clear it maintains this localization in all fully
371 differentiated cells (Djabrayan *et al*, 2014; Huynh *et al*, 2009). This, or differences in
372 microscopy techniques, could account for the inconsistency between our results and those of
373 others. Furthermore, centrosome localization and its ability to organise MTs is more likely to
374 be important at initial axon outgrowth stages, and not once the axon has already grown.
375 Regarding centrosome localization and activity in neurons, we show that axonal morphology
376 in embryos with fewer centrosomes is altered. This is the first example of a morphological
377 defect in axons associated with CL in *Drosophila*, and one we consider highly significant.
378 Under conditions of CL, we observe tortuous (wiggly) axons, suggesting that while CL does
379 not prevent neurons from extending axons, it does affect axonal outgrowth. CL could induce
380 this phenotype by disrupting the neuronal cytoskeleton and preventing MTs to form, be

severed and transported into the axons. It is known that alterations in the neuronal cytoskeleton, caused by signalling deregulation such as increased JNK activity, can result in axonal wiggliness (Karkali *et al*, 2023). Also, alterations in MT dynamics in mammalian neurons have been shown to decrease axonal elongation, but not its formation, giving rise to wiggly axons (Rochlin *et al*, 1996). In addition, axonal tortuosity is one of the hallmarks of neurodegeneration (Salvadores *et al*, 2020), which makes this phenotype a good entrance point for the analysis of the progression of various neurodegenerative diseases.

The loss of centrosome function has been documented to disrupt various developmental stages in vertebrates. In humans, CL is associated with hereditary spastic paraplegia, Bardet-Biedl syndrome, the formation of cystic kidneys, disrupted left-right asymmetry, and microcephaly (Badano *et al*, 2005; Jaiswal & Singh, 2021). Demonstrating that CL in *Drosophila* affects the development of the nervous and muscular systems paves the way for using this model organism to further explore these human diseases.

Acknowledgments

We thank M. Llimargas and J. Casanova for generously allowing us to use their laboratory for specific parts of this work and for their support throughout this study. We thank B. Estrada, C. González, K. Karkali, C. Klämbt, E. Martin-Blanco, J. Raff, S. Rumpf, Y. Zheng, the Bloomington Drosophila Stock Center (BDSC) and the Vienna Drosophila Stock Center (VDRC) for fly stocks and reagents. We extend our gratitude to Z. Novak and J. Raff for sharing two unpublished CRISPR-Cas9 made *Sas-6* fly stocks with us. Thanks also go to R. Mendez for technical assistance in all the experiments and M. Bosch for assistance and advice with confocal microscopy and software. B.G. is the recipient of a Beatriu de Pinós post-doctoral fellowship from the AGAUR (2022BP00125). This work was supported by a grant from the Spanish *Ministerio de Ciencia y Innovación* (PID2021-125860NB-I00), the Universitat de Barcelona, and a grant from the Generalitat de Catalunya (2021 SGR 1455).

Author contributions

Conceptualization: S.J.A. Methodology and Experiments: B.G., J.P., J.S.-A., J.C.-R. and S.J.A. Analysis: B.G., J.P., J.S.-A. and S.J.A. Writing: S.J.A. Reviewing and editing: S.J.A. and B.G. Supervision and Funding: S.J.A.

References

Ahmad FJ, Baas PW (1995) Microtubules released from the neuronal centrosome are transported into the axon. *Journal of Cell Science* 108 (Pt 8): 2761-2769

Anda FCd, Meletis K, Ge X, Rei D, Tsai L-H (2010) Centrosome Motility Is Essential for Initial Axon Formation in the Neocortex. *The Journal of Neuroscience* 30: 10391-10406

Anda FCd, Pollarolo G, Silva JSD, Camoletto PG, Feiguin F, Dotti CG (2005) Centrosome localization determines neuronal polarity. *Nature Cell Biology* 436: 704 - 708

Araújo SJ (2019) The Golgi Apparatus and Centriole, Functions, Interactions and Role in Disease - Centrosomes in Branching Morphogenesis. *Results Problems Cell Differ* 67: 323-336

Badano JL, Teslovich TM, Katsanis N (2005) The centrosome in human genetic disease. *Nature Reviews Genetics* 6: 194-205

Bando Y, Nomura T, Bochimoto H, Murakami K, Tanaka T, Watanabe T, Yoshida S (2015) Abnormal morphology of myelin and axon pathology in murine models of multiple sclerosis. *Neurochemistry International* 81: 16-27

Basto R, Lau J, Vinogradova T, Gardiol A, Woods CG, Khodjakov A, Raff JW (2006) Flies without centrioles. *Cell* 125: 1375-1386

Bazzi H, Anderson KV (2014) Acentriolar mitosis activates a p53-dependent apoptosis pathway in the mouse embryo. *Proc Natl Acad Sci U S A* 111: E1491-1500

Bettencourt-Dias M, Glover DM (2007) Centrosome biogenesis and function: centrosomics brings new understanding. *Nat Rev Mol Cell Biol* 8: 451-463

Bodmer R, Jan YN (1987) Morphological differentiation of the embryonic peripheral neurons in Drosophila. *Roux's Arch Dev Biol*: 69-77

Broadie K, Bate M (1993) Muscle development is independent of innervation during Drosophila embryogenesis. *Development* 119: 533-543

Castellanos E, Dominguez P, Gonzalez C (2008) Centrosome Dysfunction in Drosophila Neural Stem Cells Causes Tumors that Are Not Due to Genome Instability. *Current Biology* 18: 1209-1214

Chang W, Antoku S, Östlund C, Worman HJ, Gundersen GG (2015) Linker of nucleoskeleton and cytoskeleton (LINC) complex-mediated actin-dependent nuclear positioning orients centrosomes in migrating myoblasts. *Nucleus* 6: 77-88

Cheng T, Agwu C, Shim K, Wang B, Jain S, Mahjoub MR (2023) Aberrant centrosome biogenesis disrupts nephron and collecting duct progenitor growth and fate resulting in fibrocystic kidney disease. *Development* 150

Conduit PT, Wainman A, Raff JW (2015) Centrosome function and assembly in animal cells. *Nature Reviews Molecular Cell Biology* 16: 611-624

del Castillo U, Lu W, Winding M, Lakonishok M, Gelfand VI (2015) Pavarotti/MKLP1 regulates microtubule sliding and neurite outgrowth in Drosophila neurons. *Curr Biol* 25: 200-205

Djabrayan Nareg JV, Cruz J, de Miguel C, Franch-Marro X, Casanova J (2014) Specification of Differentiated Adult Progenitors via Inhibition of Endocycle Entry in the Drosophila Trachea. *Cell Reports* 9: 859-865

Edgar BA, O'Farrell PH (1990) The three postblastoderm cell cycles of Drosophila embryogenesis are regulated in G2 by string. *Cell* 62: 469-480

Fatalska A, Stepinac E, Richter M, Kovacs L, Pietras Z, Puchinger M, Dong G, Dadlez M, Glover DM (2021) The dimeric Golgi protein Gorab binds to Sas6 as a monomer to mediate centriole duplication. *Elife* 10

Fujioka M, Lear BC, Landgraf M, Yusibova GL, Zhou J, Riley KM, Patel NH, Jaynes JB (2003) Even-skipped, acting as a repressor, regulates axonal projections in Drosophila. *Development* 130: 5385-5400

Gartenmann L, Vicente CC, Wainman A, Novak ZA, Sieber B, Richens JH, Raff JW (2020) Drosophila Sas-6, Ana2 and Sas-4 self-organise into macromolecular structures that can be used to probe centriole and centrosome assembly. *Journal of Cell Science* 133: jcs244574

Ghysen A, Dambly-Chaudière C, Aceves E, Jan L, Jan Y (1986) Sensory neurons and peripheral pathways in Drosophila embryos. *Rouxs Arch Dev Biol* 195: 281-289

Gogendeau D, Basto R (2010) Centrioles in flies: The exception to the rule? *Semin Cell Dev Biol* 21: 163-173

Gomes ER, Jani S, Gundersen GG (2005) Nuclear Movement Regulated by Cdc42, MRCK, Myosin, and Actin Flow Establishes MTOC Polarization in Migrating Cells. *Cell* 121: 451-463

Goundiam O, Basto R (2020) Centrosomes in disease: how the same music can sound so different? *Current opinion in structural biology* 66: 74-82

Grzonka M, Bazzi H (2024) Mouse SAS-6 is required for centriole formation in embryos and integrity in embryonic stem cells. *eLife* 13: e94694

Harrison RG (1910) The outgrowth of the nerve fiber as a mode of protoplasmic movement. *Journal of Experimental Zoology* 9: 787-846

Hartenstein V (1988) Development of Drosophila larval sensory organs: spatiotemporal pattern of sensory neurones, peripheral axonal pathways and sensilla differentiation. *Development* 102: 869-886

Hartenstein V, Rudloff E, Campos-Ortega JA (1987) The pattern of proliferation of the neuroblasts in the wild-type embryo of Drosophila melanogaster. *Rouxs Arch Dev Biol* 196: 473-485

Hummel T, Krukkert K, Roos J, Davis G, Klämbt C (2000) Drosophila Futsch/22C10 Is a MAP1B-like Protein Required for Dendritic and Axonal Development. *Neuron* 26: 357-370

Huynh MA, Stegmüller J, Litterman N, Bonni A (2009) Regulation of Cdh1-APC function in axon growth by Cdh1 phosphorylation. *J Neurosci* 29: 4322-4327

Jacobs J, Goodman C (1989) Embryonic development of axon pathways in the Drosophila CNS. II. Behavior of pioneer growth cones. *The Journal of Neuroscience* 9: 2412-2422

Jaiswal S, Singh P (2021) Centrosome dysfunction in human diseases. *Semin Cell Dev Biol* 110: 113-122

Jana SC, Bettencourt-Dias M, Durand B, Megraw TL (2016) Drosophila melanogaster as a model for basal body research. *Cilia*: 1-7

Jeong S (2021) Molecular Mechanisms Underlying Motor Axon Guidance in Drosophila. *Molecules and Cells* 44: 549-556

Karkali K, Vernon SW, Baines RA, Panayotou G, Martín-Blanco E (2023) Puckered and JNK signaling in pioneer neurons coordinates the motor activity of the Drosophila embryo. *Nature Communications* 14: 8186

Kopeć S (1928) On the Influence of Intermittent Starvation on the Longevity of the Imaginal Stage of Drosophila Melanogaster. *Journal of Experimental Biology* 5: 204-211

Kushner EJ, Ferro LS, Liu J-Y, Durrant JR, Rogers SL, Dudley AC, Bautch VL (2014) Excess centrosomes disrupt endothelial cell migration via centrosome scattering. *J Cell Biol* 206: 257-272

Leask A, Obrietan K, Stearns T (1997) Synaptically coupled central nervous system neurons lack centrosomal γ-tubulin. *Neuroscience Letters* 229: 17-20

Leidel S, Gönczy P (2003) SAS-4 is essential for centrosome duplication in C elegans and is recruited to daughter centrioles once per cell cycle. *Dev Cell* 4: 431-439

Lin T-c, Neuner A, Schiebel E (2015) Targeting of γ-tubulin complexes to microtubule organizing centers: conservation and divergence. *Trends in Cell Biology* 25: 296-307

Lindhout FW, Portegies S, Kooistra R, Herstel LJ, Stucchi R, Hummel JJA, Scheefhals N, Katrukha EA, Altelaar M, MacGillavry HD *et al* (2021) Centrosome-mediated microtubule remodeling during axon formation in human iPSC-derived neurons. *The EMBO Journal* 40: e106798

Loh M, Bernard F, Guichet A (2023) Kinesin-1 promotes centrosome clustering and nuclear migration in the Drosophila oocyte. *Development* 150

Marmion RA, Simpkins AG, Barrett LA, Denberg DW, Zusman S, Schottenfeld-Roames J, Schüpbach T, Shvartsman SY (2023) Stochastic phenotypes in RAS-dependent developmental diseases. *Current Biology* 33: 807-816.e804

Marthiens V, Rujano MA, Pennetier C, Tessier S, Paul-Gilloteaux P, Basto R (2013) Centrosome amplification causes microcephaly. *Nat Cell Biol* 15: 731-740

Martin V, Mrkusich E, Steinel MC, Rice J, Merritt DJ, Whitington PM (2008) The L1-type cell adhesion molecule Neuroglian is necessary for maintenance of sensory axon advance in the Drosophila embryo. *Neural Dev* 3: 10

Meghini F, Martins T, Tait X, Fujimitsu K, Yamano H, Glover DM, Kimata Y (2016) Targeting of Fzr/Cdh1 for timely activation of the APC/C at the centrosome during mitotic exit. *Nat Commun* 7: 12607

Meka DP, Kobler O, Hong S, Friedrich CM, Wuesthoff S, Henis M, Schwanke B, Krisp C, Schmuelling N, Rueter R *et al* (2022) Centrosome-dependent microtubule modifications set the conditions for axon formation. *Cell Reports* 39: 110686

Merritt DJ, Whitington PM (1995) Central projections of sensory neurons in the Drosophila embryo correlate with sensory modality, soma position, and proneural gene function. *J Neurosci* 15: 1755-1767

Metzger T, Gache V, Xu M, Cadot B, Folker ES, Richardson BE, Gomes ER, Baylies MK (2012) MAP and kinesin-dependent nuclear positioning is required for skeletal muscle function. *Nature* 484: 120-124

Nabel-Rosen H, Toledano-Katchalski H, Volohonsky G, Volk T (2005) Cell Divisions in the Drosophila Embryonic Mesoderm Are Repressed via Posttranscriptional Regulation of string/cdc25 by HOW. *Current Biology* 15: 295-302

Nguyen MM, Stone MC, Rolls MM (2011) Microtubules are organized independently of the centrosome in Drosophila neurons. *Neural Development* 6: 38

Pearl R, Parker SL (1921) Experimental Studies on the Duration of Life. I. Introductory Discussion of the Duration of Life in Drosophila. *Am Nat* 55: 481-509

Peel N, Stevens NR, Basto R, Raff JW (2007) Overexpressing Centriole-Replication Proteins In Vivo Induces Centriole Overduplication and De Novo Formation. *Current Biology* 17: 834-843

Poulton John S, Cuningham John C, Peifer M (2014) Acentrosomal Drosophila Epithelial Cells Exhibit Abnormal Cell Division, Leading to Cell Death and Compensatory Proliferation. *Developmental Cell* 30: 731-745

Poulton JS, Cuningham JC, Peifer M (2017) Centrosome and spindle assembly checkpoint loss leads to neural apoptosis and reduced brain size. *Journal of Cell Biology* 216: 1255-1265

Ricolo D, Castro-Ribera J, Araújo SJ (2021) Cytoskeletal players in single-cell branching morphogenesis. *Developmental Biology* 477: 22-34

Ricolo D, Deligiannaki M, Casanova J, Araújo SJ (2016) Centrosome Amplification Increases Single-Cell Branching in Post-mitotic Cells. *Curr Biol* 26: 2805-2813

Rochlin MW, Wickline KM, Bridgman PC (1996) Microtubule Stability Decreases Axon Elongation but Not Axoplasm Production. *The Journal of Neuroscience* 16: 3236-3246

Salvadores N, Gerónimo-Olvera C, Court FA (2020) Axonal Degeneration in AD: The Contribution of Aβ and Tau. *Front Aging Neurosci* 12: 581767

Sanchez-Huertas C, Freixo F, Viais R, Lacasa C, Soriano E, Luders J (2016) Non-centrosomal nucleation mediated by augmin organizes microtubules in post-mitotic neurons and controls axonal microtubule polarity. *Nat Commun* 7: 12187

564 Sánchez-Soriano N, Prokop A (2005) The influence of pioneer neurons on a growing motor
565 nerve in Drosophila requires the neural cell adhesion molecule homolog FasciclinII. *J*
566 *Neurosci* 25: 78-87
567 Schnorrer F, Schönbauer C, Langer CCH, Dietzl G, Novatchkova M, Schernhuber K, Fellner
568 M, Azaryan A, Radolf M, Stark A *et al* (2010) Systematic genetic analysis of muscle
569 morphogenesis and function in Drosophila. *Nature* 464: 287-291
570 Stevens NR, Raposo AASF, Basto R, Johnston DS, Raff JW (2007) From Stem Cell to
571 Embryo without Centrioles. 17: 1498-1503
572 Stiess M, Maghelli N, Kapitein LC, Gomis-Rüth S, Wilsch-Bräuninger M, Hoogenraad CC,
573 Tolić-Nørrelykke IM, Bradke F (2010) Axon extension occurs independently of centrosomal
574 microtubule nucleation. *Science* 327: 704-707
575 Tillery MML, Blake-Hedges C, Zheng Y, Buchwalter RA, Megraw TL (2018) Centrosomal and
576 Non-Centrosomal Microtubule-Organizing Centers (MTOCs) in Drosophila melanogaster.
577 *Cells* 7
578 Varmark H, Llamazares S, Rebollo E, Lange B, Reina J, Schwarz H, Gonzalez C (2007)
579 Asterless is a centriolar protein required for centrosome function and embryo development in
580 Drosophila. *Curr Biol* 17: 1735-1745
581 Younossi-Hartenstein A, Hartenstein V (1993) The role of the tracheae and musculature
582 during pathfinding of Drosophila embryonic sensory axons. *Dev Biol* 158: 430-447
583 Yu W, Centonze VE, Ahmad FJ, Baas PW (1993) Microtubule nucleation and release from
584 the neuronal centrosome. *The Journal of cell biology* 122: 349-359
585

586 **Figure legends**

587

588 **Fig. 1 – *Sas-4* loss of function induces axonal misrouting defects.**

589 (A) *Sas-4* adult fly at 6h after eclosion. (B) Graphical representation of the percentage of *Sas-*
590 *4* surviving individuals at different life cycle stages. (C) Highlight of the three main FasII
591 positive nerves over a microscope image of two embryonic lateral segments. (D-G) Details of
592 three segments from stage 16 embryos stained with anti-FasII antibody; scale bar 10 µm. (D'-
593 G') Confocal lateral views of stage 16 embryos stained with anti-FasII antibody; scale bar 50
594 µm. (H) Penetrance and expressivity of the ISN mutant phenotypes in different *Sas-4* mutant
595 conditions; control is *w* (n=35); *Sas-4*^{s2214} (n=53); *Sas-4*^{s2214}*/Df* (n=25); *RN2Gal4xUASSas-*
596 *4RNAi* (n=15); *UbqSas-4GFP;Sas-4/Df* (n=28). (I-L) Details of three segments from stage 16
597 embryos stained with anti-Futsch antibody; scale bar 5 µm (I'-L') Confocal lateral views of
598 stage 16 embryos stained with anti-Futsch antibody; scale bar 50 µm. (H) Penetrance and
599 expressivity of the sensory axon mutant phenotypes in different *Sas-4* mutant conditions;
600 control is *Sas-4/+* (n=20); *Sas-4*^{s2214} (n=20); *Sas-4*^{s2214}*/Df* (n=20); *P0163Gal4xUASSas-4RNAi*
601 (n=20); *UbqSas-4GFP;Sas-4/Df* (n=20).

602

603 **Fig. 2 - *Sas-4* loss of function induces muscle defects.**

604 (A,B) Stage 16 embryos stained with an antibody against myosin to mark the embryonic
605 muscle structure in green. (A-A') Control embryo and (B-B') *Sas-4* mutant embryo. (C)
606 Schematic representation of the motor axon muscle innervation pattern of a wt (wt) and *Sas-*
607 *4* mutant embryo of *Drosophila*. TN, transverse nerve; ISN, intersegmental nerve, and SN,
608 segmental nerve. (D-H) Confocal projections of four segments from stage 16 embryos of
609 different mutant conditions stained with anti-myosin (green and D') and anti-FasII (magenta
610 and D'') antibodies; scale bar 10 µm. (D''-H'') composite images with the two channels (anti-
611 myosin in green and anti-FasII in magenta). (D'''-H''') Myosin-stained muscle single-stacks.
612 Scale bar 10 µm. (I) Penetrance and expressivity of the ISN mutant phenotypes in different
613 *Sas-4* mutant conditions; control is *Sas-4/+* (n=27); *Sas-4*^{s2214} (n=27); *Sas-4*^{s2214}*/Df* (n=25);
614 *Mef2Gal4xUASSas-4RNAi* (n=19); *RN2Gal4xUASSas-4RNAi* (n=15). (J) Penetrance and
615 expressivity of the muscle mutant phenotypes in different *Sas-4* mutant conditions; control is
616 *w* (n=16); *Sas-4*^{s2214} (n=16); *Sas-4*^{s2214}*/Df* (n=10); *Mef2Gal4xUASSas-4RNAi* (n=10);
617 *RN2Gal4xUASSas-4RNAi* (n=10).

618

619 **Fig. 3 - *Sas-6* loss of function induces axonal misrouting and muscle defects.**

620 (A) *Sas-6* adult fly at 6h after eclosion. (B) Quantification of the number of centrioles per stage
621 16 embryonic segmental area in Control, *Sas-6/+* embryos, (mean 165.9 ± 26.4, n=10) and
622 *Sas-6* embryos displaying PNS mutant phenotypes (mean 53.2 ± 21.9, n=15); unpaired t-test
623 with Welch's correction $p<0.0001$. (C) Graphical representation of the percentage of *Sas-6*
624 surviving individuals at different life-cycle stages. (D) Penetrance and expressivity of the ISN
625 mutant phenotypes in *Sas-6* embryos; controls are *Sas-6*$^{\Delta a}$ (n=19) and *Sas-6*$^{\Delta b}$ (n=8); mutants
626 are *Sas-6*$^{\Delta a/\Delta b}$ (n=42). (E, F) Confocal projections of four segments from stage 16 embryos of
627 control and *Sas-6*$^{\Delta a/\Delta b}$ mutants stained with anti-myosin (magenta and E', F') and anti-FasII
628 (green and E, F) antibodies. (E''-F'') Composite projections with the two channels; scale bar

629 is 10 µm. (E'''-F''') Composite projections of the two channels showing the whole embryo;
630 scale bar is 50µm.
631
632 **Fig. 4 - Pioneer neurons have centrioles localizing to the sites of axon outgrowth**
633 (A) Confocal image showing 3 segments of the embryonic Ventral Nerve Cord (VNC) midline
634 marked with an antibody against FasII and GFP driven by the RN2 driver marking the aCC,
635 pCC and RP2 in green. (B) Confocal section showing an aCC neuron and its centriole at the
636 axonal exit point, marked with an antibody against CP309; quantification of centrioles present
637 in different aCC quadrants and the percentage of aCC with centrioles present at the axonal
638 exit point (72%, n=75). (C, D) CP309 marking all centrioles and the neuronal body drawn from
639 the channel marking the neuron (C', D'). (C'') aCC+pCC and RP2 (D'') marked in green and
640 CP309 in magenta. Scale bar is 5µm. (G) Quantification of centriole numbers in control and
641 *Sas-4* aCC+pCC and RP2 pioneer neurons; Control RP2 average 0.81 (n=22), control
642 aCC+pCC average 2.53 (n=41), *Sas-4* RP2 average 0.26 (n=34) and *Sas-4* aCC+pCC
643 average 0.87 (n=38); unpaired t-test with Welch's correction control RP2 vs *Sas-4* RP2
644 p=0.0005, control aCC+pCC vs *Sas-4* aCC+pCC p<0.0001.
645
646 **Fig. 5 – Non-ciliated sensory neurons have centrioles**
647 (A) Dorsal cluster neurons in a stage 15 embryo marked with anti-Futsch (22C10) in magenta
648 to mark the sensory neurons and Asterless (Asl) in green to mark the centrioles. (A') Inverted
649 channels with neurons identified and (A'') cell bodies drawn to show the centrioles within each
650 neuron. Scale bar is 8 µm (B) Stage 16 dorsal cluster with the neurons identified and ddaC
651 marked in green with ppkGAL4 driving UASCD8GFP marking class IV dendritic arborisation
652 neurons, with centriole in cyan and Futsch in green. Scale bar is 5 µm. Quantification of the
653 number of ddaC neurons with centrioles (81.4% n=43). (C) Control and (D,E) dorsal clusters
654 marked with Futsch in magenta CP309 in green. (C', D' and E') CP309 marking all
655 centrosomes and cell bodies drawn from the other channel (C'', D'' and E''). (F) Quantification
656 of the number of centrioles per stage 16 embryonic segmental area in Control, *Sas-4/+*

657 embryos, (mean 179.4 ± 30.1, n=25), *Sas-4* embryos displaying PNS mutant phenotypes
658 (mean 68.2 ± 21.6, n=23), *Sas-4* embryos without mutant phenotypes (mean 86.3 ± 23.8,
659 n=24) and *Sas-4* embryos rescued by ubiquitous expression of Sas-4 (mean 157.3 ± 51.45,
660 n=23); unpaired t-test with Welch's correction control vs *Sas-4* p<0.0001, control vs *Sas-4* no
661 defects p<0.0001, control vs *Sas-4* rescue p=0.08 and *Sas-4* vs *Sas-4* no defects p=0.009.
662
663 **Fig. 6 – Pioneer motor neurons have active centrosomes**
664 (A) aCC+pCC and RP2 (B) marked in green, CP309 in magenta and ace-tub in blue; scale
665 bar 5 µm. (A', B') CP309 marking all centrioles and the neuronal body drawn from the channel
666 marking the neuron (A, B). (A'', B'') CP309 marking all centrioles and ace-tub antibody marking
667 stable MTs with the neuronal body drawn from the channel marking the neuron (A, B). (C)
668 aCC+pCC and RP2 (D) marked in green, CP309 in magenta and γ-tub in blue. (C', D') CP309
669 marking all centrioles and the neuronal body drawn from the channel marking the neuron (C,
670 D). (C'', D'') CP309 marking all centrioles and ace-tub antibody marking stable MTs with the
671 neuronal body drawn from the channel marking the neuron (C, D). (E) Quantification of the
672 total number of centrioles in aCC+pCC and RP2 neurons and quantification of the numbers of
673 these which colocalize with γ-tub (n=18).
674
675 **Fig. 7 - *Sas-4* loss of function induces wiggly axon phenotypes**
676 (A-E) Confocal images of stage 16 RN2GAL4, UASCD8GFP embryonic lateral segments
677 (A,B) or the ventral midline (C-F) in wt (A, C) or *Sas-4* mutant background (B, D, E). (A',B')
678 axons marked with anti-FasII and (A'', B'', D, E) axons marked with anti-GFP, detecting the
679 axonal membranes. Scale bar is 10 µm in A-B and x µm in C-E. (F) Quantification of the
680 proportion (wiggly/normal axons) of wiggly axons in control and *Sas-4* mutant aCC and RP2
681 neurons; Mann-Whitney test p=0.025 in control vs *Sas-4* aCC (n=8 embryos) and p=0.0065
682 in control vs *Sas-4* RP2 (n=8 embryos). (G) Schematic representation of the wiggly axon

683 phenotypes; in Sas-4 aCC and RP2 neurons, the absence of active centrosomes gives rise to

684 axonal tortuosity.

685

Fig. 1

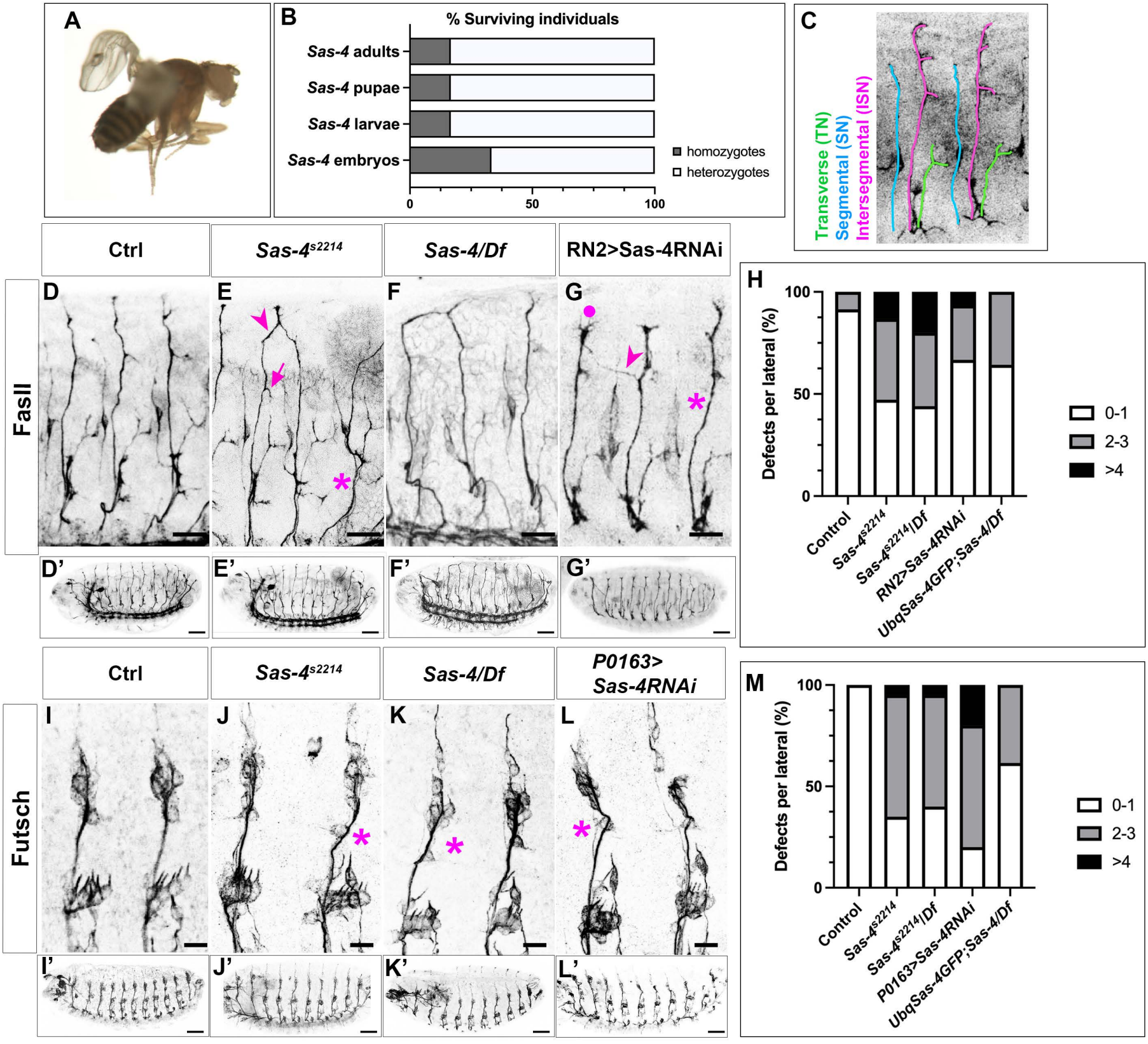
A
B
% Surviving individuals
Sas-4 adults
Sas-4 pupae
Sas-4 larvae
Sas-4 embryos
homozygotes
heterozygotes
0
50
100
C
Transverse (TN)
Segmental (SN)
Intersegmental (ISN)
Ctrl
Sas-4s2214
Sas-4/Df
RN2>Sas-4RNAi
FasII
D
E
F
G
D'
E'
F'
G'
H
Defects per lateral (%)
100
50
0
Control
Sas-4s2214
Sas-4s2214/Df
RN2>Sas-4RNAi
UbqSas-4GFP;Sas-4/Df
0-1
2-3
>4
Ctrl
Sas-4s2214
Sas-4/Df
P0163>
Sas-4RNAi
Futsch
I
J
K
L
I'
J'
K'
L'
M
Defects per lateral (%)
100
50
0
Control
Sas-4s2214
Sas-4s2214/Df
P0163>Sas-4RNAi
UbqSas-4GFP;Sas-4/Df
0-1
2-3
>4

Fig 2

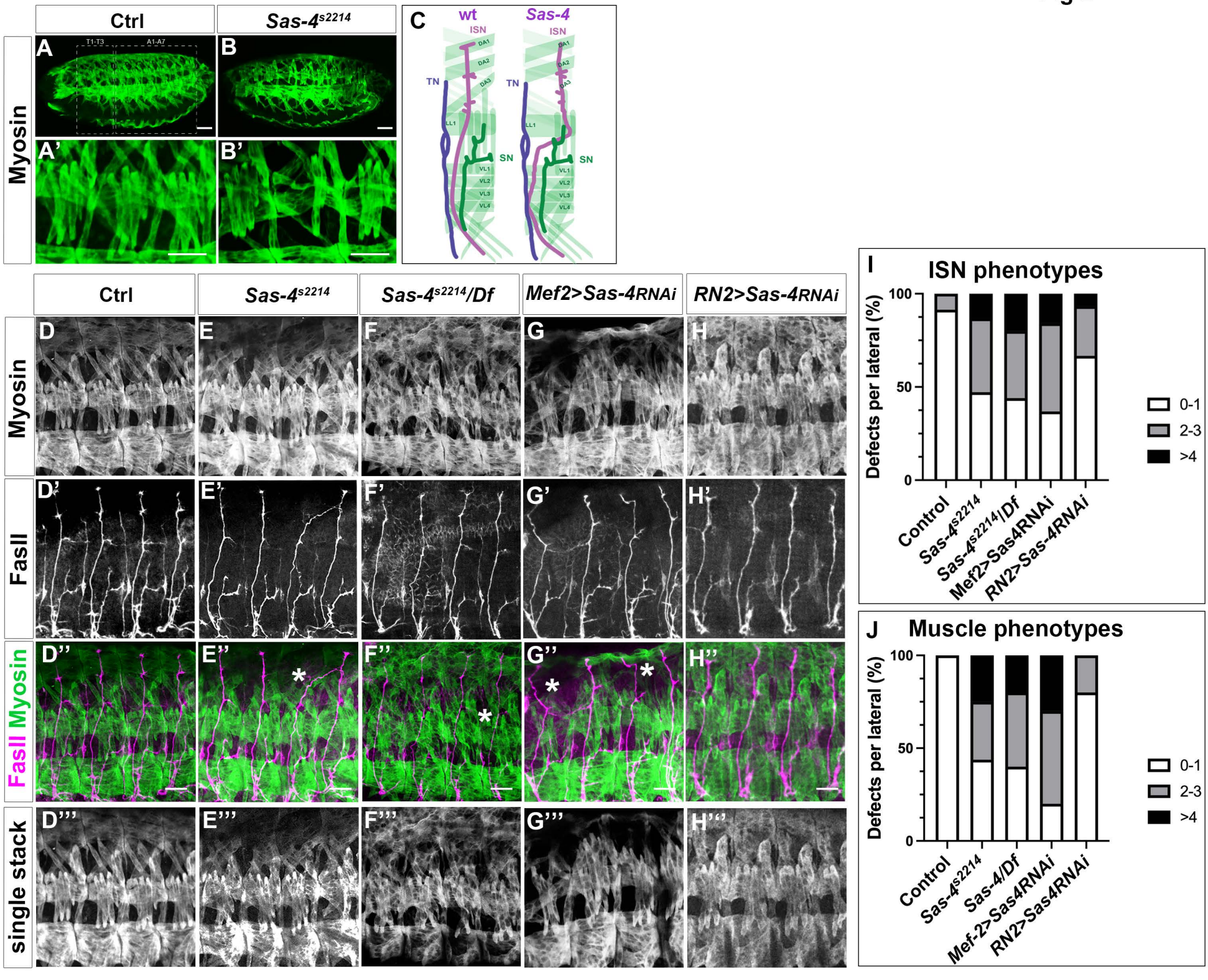
Ctrl
Sas-4s2214
Myosin
A
B
A'
B'
T1-T3
A1-A7
C
wt
Sas-4
ISN
TN
SN
DA1
DA2
DA3
LL1
VL1
VL2
VL3
VL4
Ctrl
Sas-4s2214
Sas-4s2214/Df
Mef2>Sas-4RNAi
RN2>Sas-4RNAi
Myosin
FasII
FasII Myosin
single stack
D
E
F
G
H
D'
E'
F'
G'
H'
D''
E''
F''
G''
H''
D'''
E'''
F'''
G'''
H'''
I
ISN phenotypes
Defects per lateral (%)
100
50
0
Control
Sas-4s2214
Sas-4s2214/Df
Mef2>Sas4RNAi
RN2>Sas-4RNAi
0-1
2-3
>4
J
Muscle phenotypes
Defects per lateral (%)
100
50
0
Control
Sas-4s2214
Sas-4/Df
Mef-2>Sas4RNAi
RN2>Sas4RNAi
0-1
2-3
>4

Fig. 3

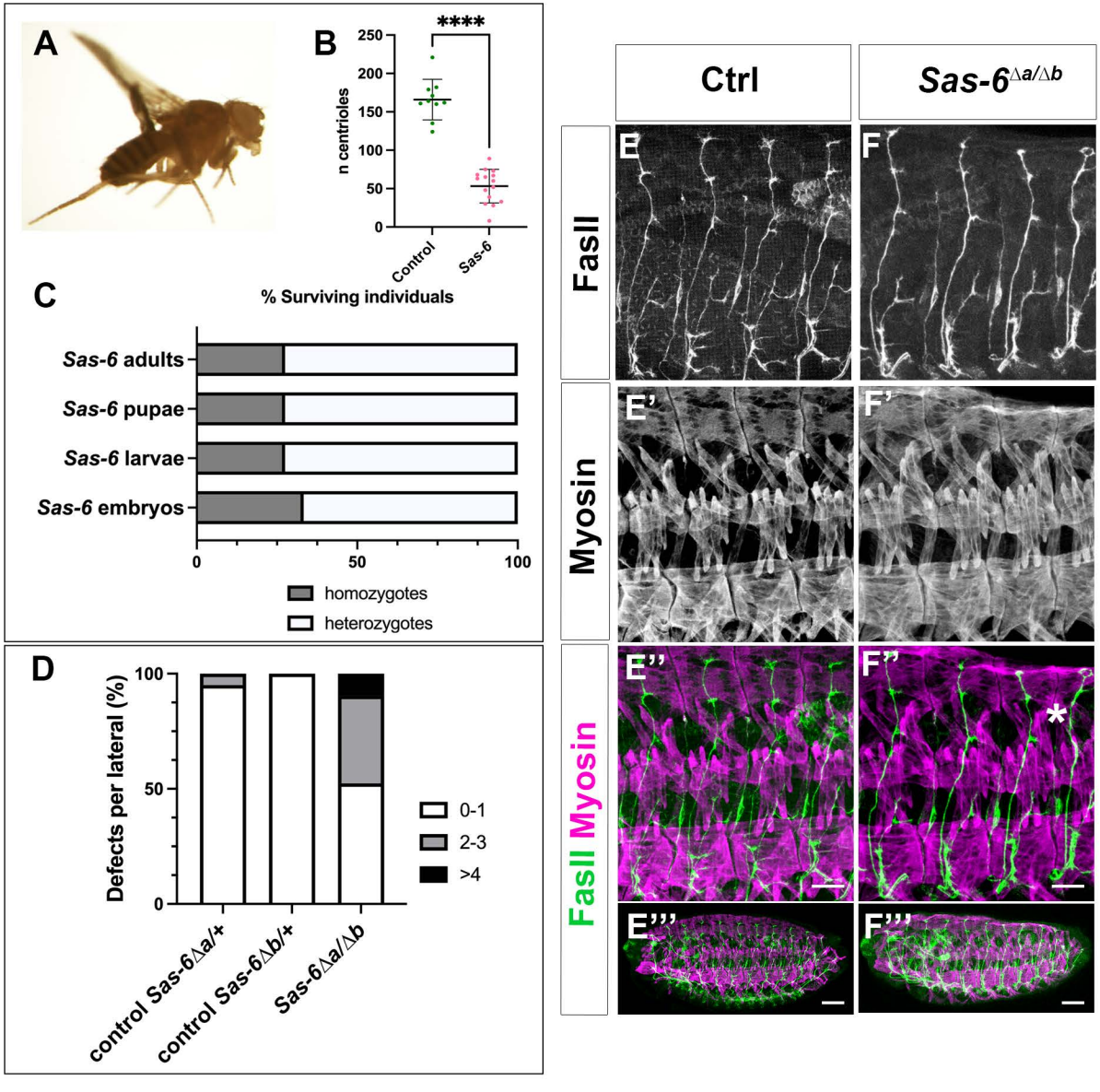
A
B
****
n centrioles
250
200
150
100
50
0
Control
Sas-6
C
% Surviving individuals
Sas-6 adults
Sas-6 pupae
Sas-6 larvae
Sas-6 embryos
0
50
100
homozygotes
heterozygotes
D
Defects per lateral (%)
100
50
0
0-1
2-3
>4
control Sas-6Δa/+
control Sas-6Δb/+
Sas-6Δa/Δb
Ctrl
Sas-6Δa/Δb
FasII
Myosin
FasII Myosin
E
F
E'
F'
E''
F''
E'''
F'''
*

Fig. 4

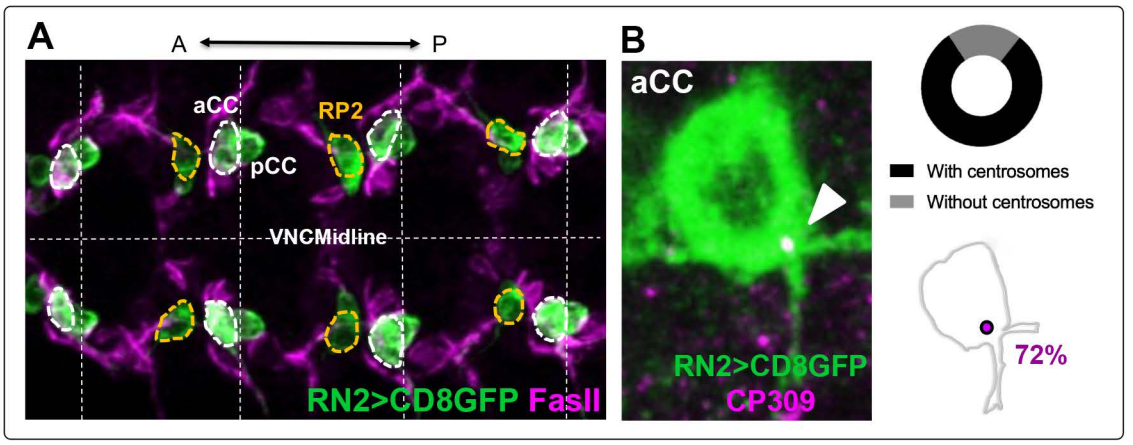
A
A
P
aCC
RP2
pCC
VNCMidline
RN2>CD8GFP FasII
B
aCC
RN2>CD8GFP
CP309
With centrosomes
Without centrosomes
72%

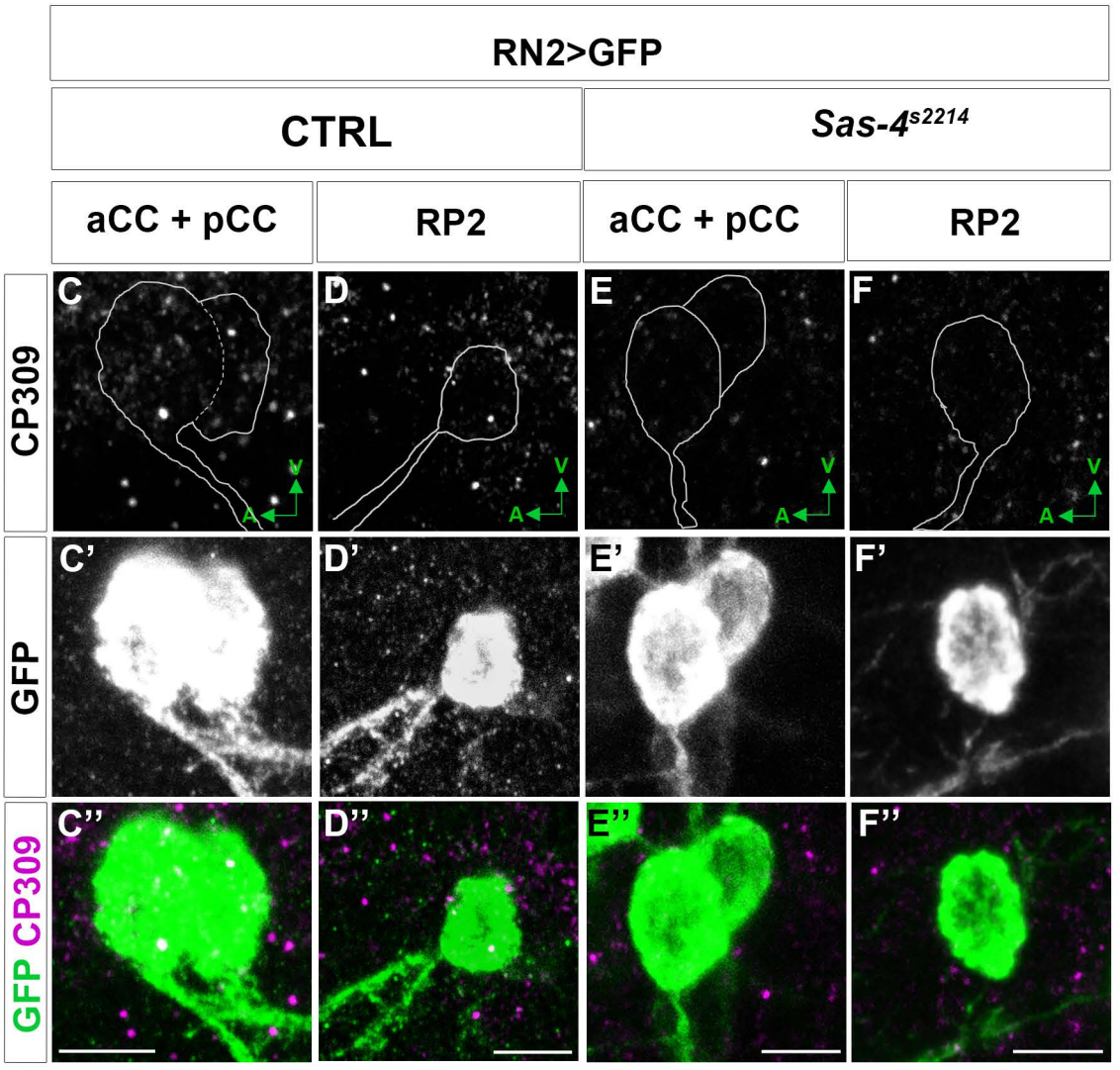
RN2>GFP
CTRL
Sas-4s2214
aCC + pCC
RP2
aCC + pCC
RP2
CP309
GFP
GFP CP309
C
D
E
F
C'
D'
E'
F'
C''
D''
E''
F''
V
A

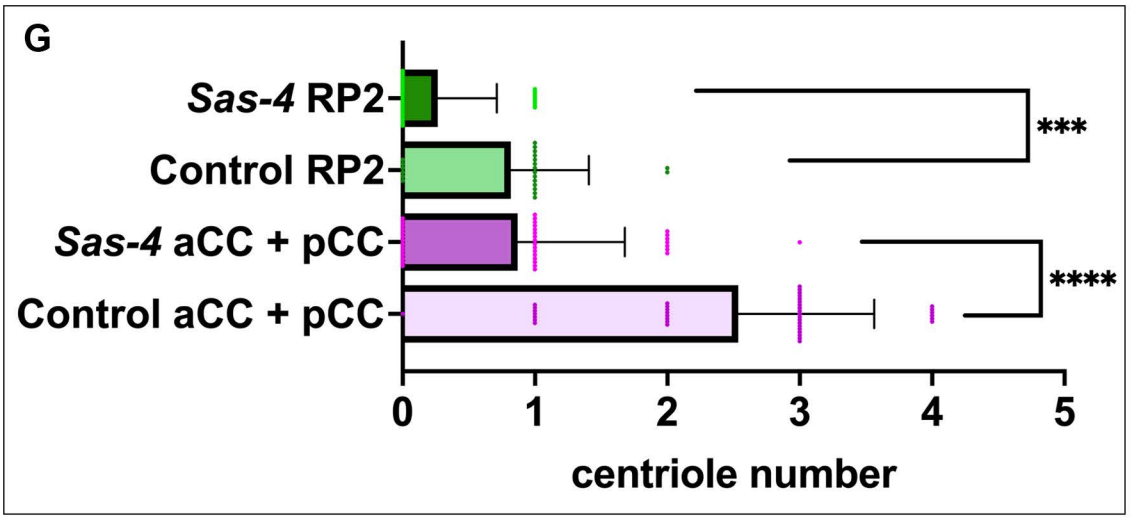
G
Sas-4 RP2
Control RP2
Sas-4 aCC + pCC
Control aCC + pCC
***
****
0
1
2
3
4
5
centriole number

Fig. 5

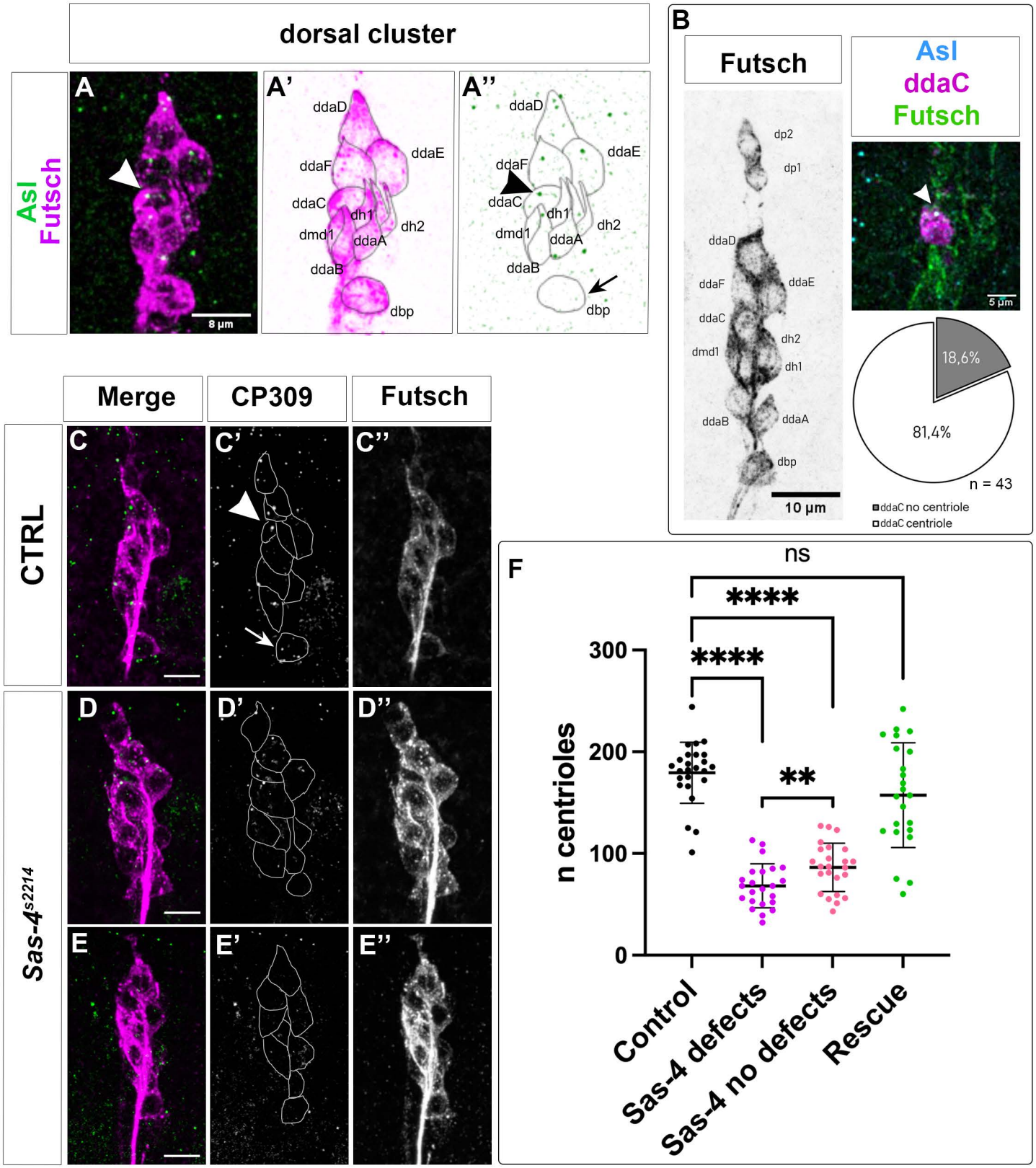
dorsal cluster
Asl
Futsch
A
A'
A''
ddaD
ddaE
ddaF
ddaC
dh1
dh2
dmd1
ddaA
ddaB
dbp
8 µm
B
Futsch
Asl
ddaC
Futsch
dp2
dp1
10 µm
5 µm
18,6%
81,4%
n = 43
ddaC no centriole
ddaC centriole
Merge
CP309
Futsch
CTRL
Sas-4s2214
C
C'
C''
D
D'
D''
E
E'
E''
F
ns
****
****
**
n centrioles
300
200
100
0
Control
Sas-4 defects
Sas-4 no defects
Rescue

Fig. 6

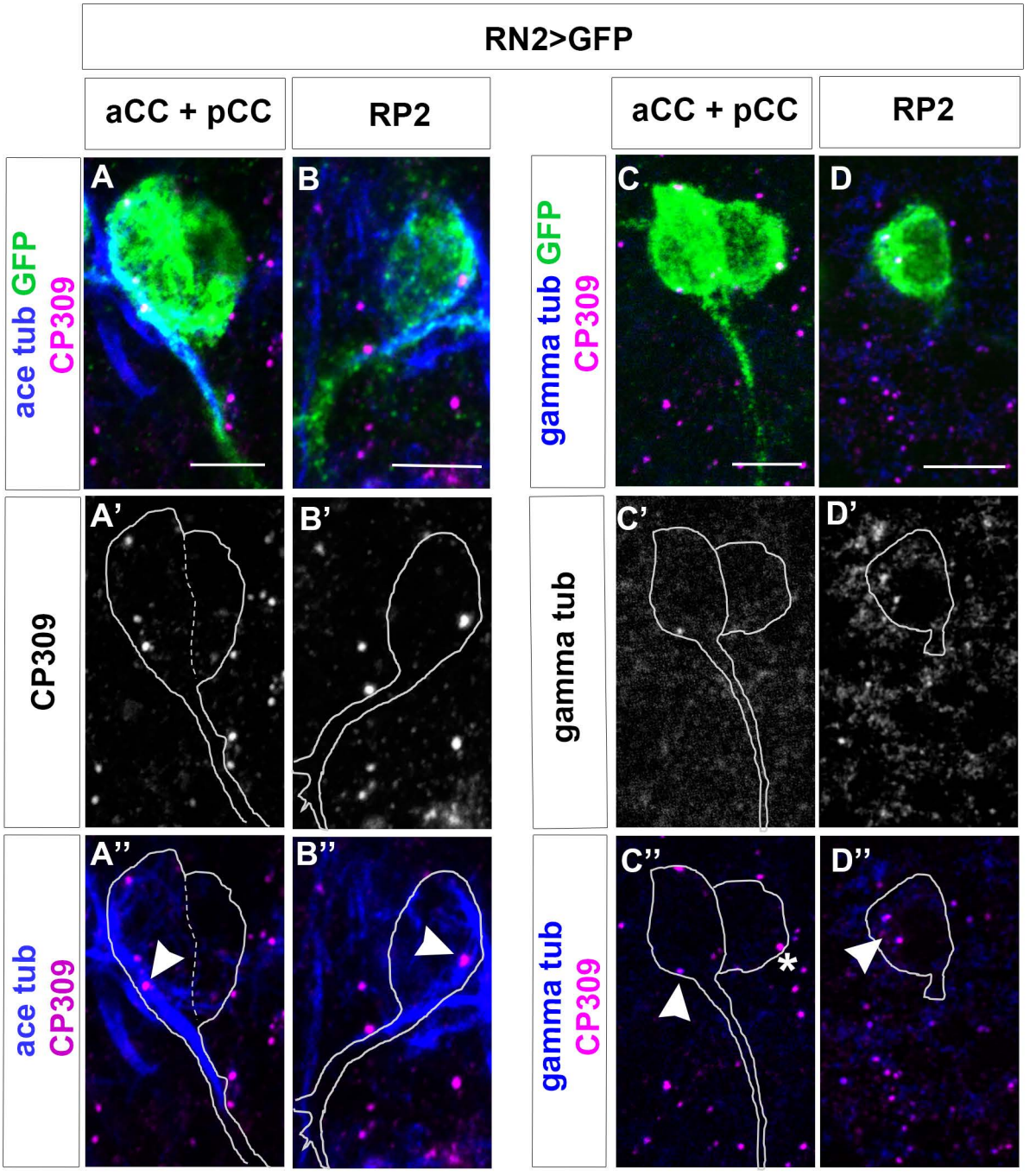
RN2>GFP
aCC + pCC
RP2
aCC + pCC
RP2
ace tub GFP
CP309
gamma tub GFP
CP309
CP309
gamma tub
ace tub
CP309
gamma tub
CP309
A
B
C
D
A'
B'
C'
D'
A''
B''
C''
D''
*

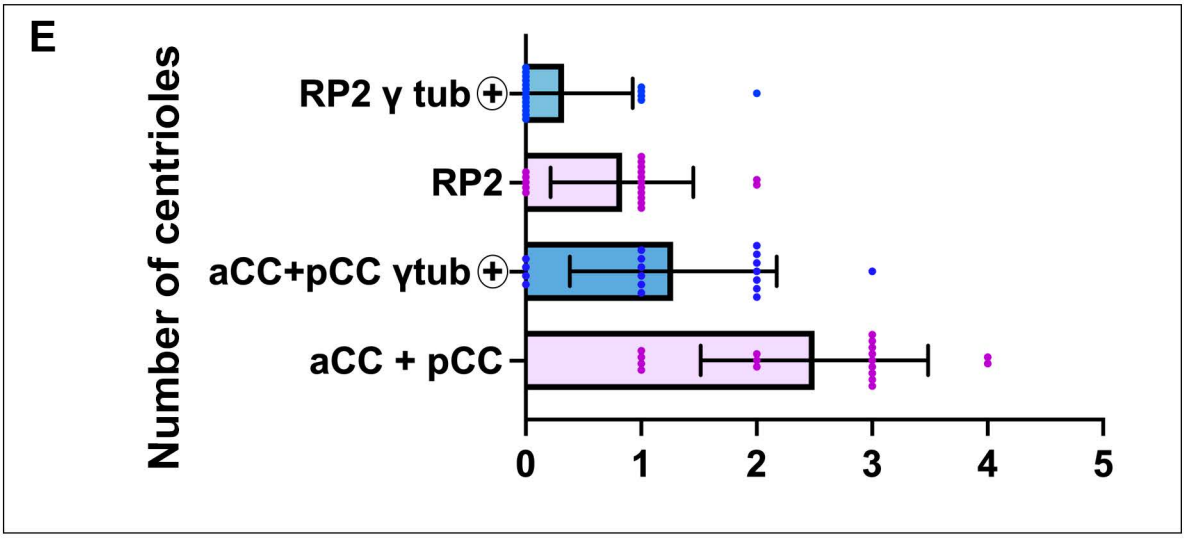
E
Number of centrioles
RP2 γ tub ⊕
RP2
aCC+pCC γtub ⊕
aCC + pCC
0
1
2
3
4
5

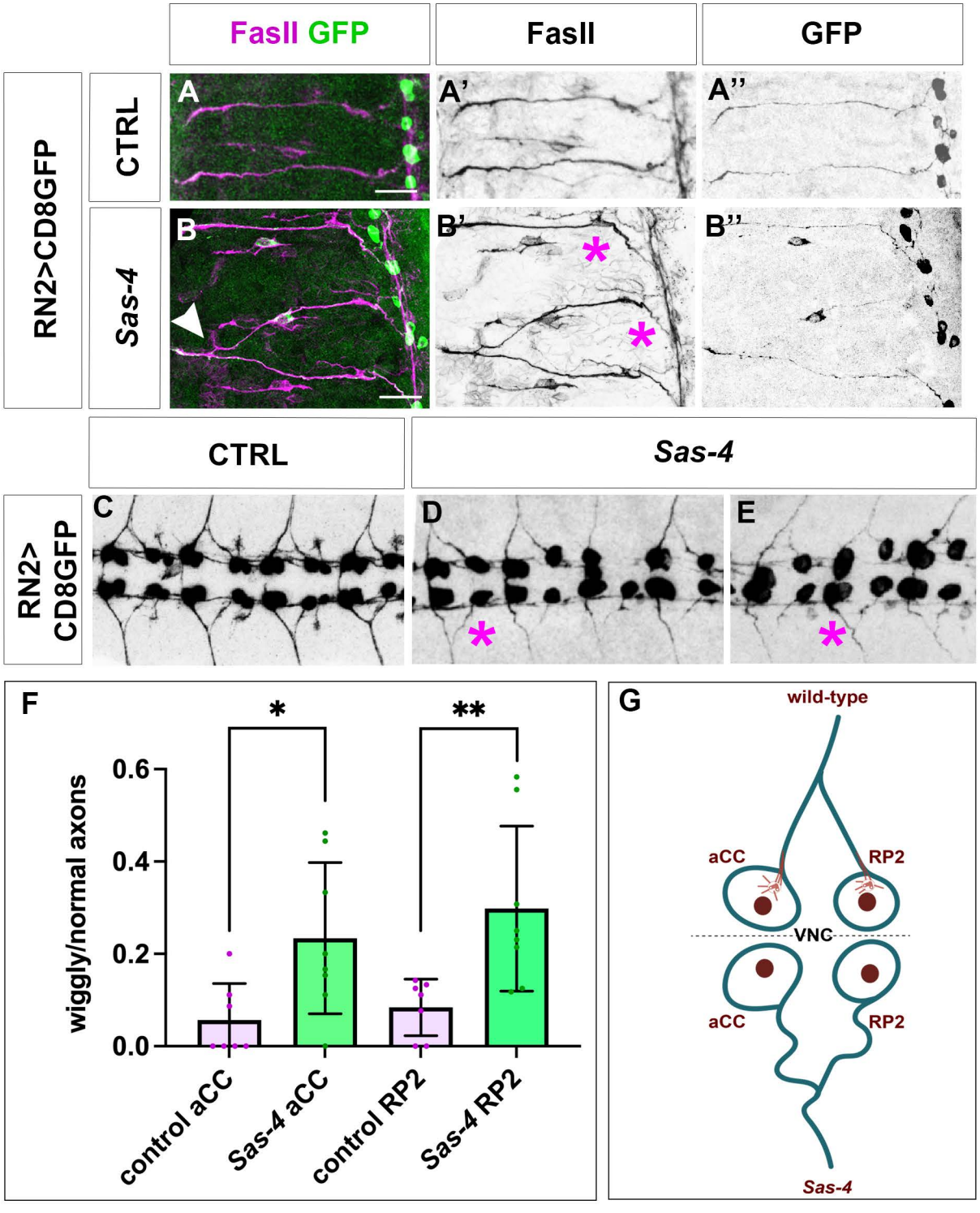
FasII GFP
FasII
GFP
RN2>CD8GFP
CTRL
Sas-4
A
A'
A''
B
B'
B''
CTRL
Sas-4
RN2> CD8GFP
C
D
E
F
wiggly/normal axons
0.6
0.4
0.2
0.0
*
**
control aCC
Sas-4 aCC
control RP2
Sas-4 RP2
G
wild-type
aCC
RP2
VNC
aCC
RP2
Sas-4